Journal of Applied Electrochemistry (2005) 35:1183–1190
DOI 10.1007/s10800-005-9029-3

Simplified model to predict the effect of the leakage current on primary and secondary current distributions in electrochemical reactors with a bipolar electrode

E.R. HENQUÍN and J.M. BISANG*
Programa de Electroquímica Aplicada e Ingeniería Electroquímica (PRELINE), Facultad de Ingeniería Química (UNL), Santiago del Estero 2829, S3000AOM Santa Fe, Argentina
*(*author for correspondence, e-mail: jbisang@fiqus.unl.edu.ar)*

Received 19 November 2004; accepted in revised form 12 July 2005

Key words: bipolar electrodes, current distribution, electrochemical reactors, leakage current

Abstract

A simplified mathematical model to calculate the current distributions in bipolar electrochemical reactors is proposed. The current distributions are deduced from a combination of the voltage balance in the reactor with a voltage balance including the electrolyte inlet and outlet. Thus, equations to predict the effect of geometric and operational variables on the current distributions at the electrodes are reported. The parameters acting upon the current distributions were lumped into two dimensionless variables and their effects on the current distributions are discussed. The primary current distributions are obtained as a limiting case. Comparisons between calculated and experimental primary current distributions are reported.

List of symbols

A	transverse section of the electrolyte manifold (m^2)
b_i	constant in the Tafel equation of the ith reaction (i = a or c) (V)
C_1	constant given by Equation 7 (V)
C_2	constant given by Equation 13 (V)
$\overline{d}_r$	mean relative deviation (%)
e	interelectrode distance (m)
G	length of the electrolyte manifold (m)
j	current density (A m^{-2})
$\overline{j}$	average current density at Δy (A m^{-2})
$j_{0,\,i}$	exchange current density of the ith reaction (i = a or c) (A m^{-2})
$j_{i,\,j}$	current density of the ith reaction (i = a or c) at the jth electrode (j = A, B or C) (A m^{-2})
I	total current (A)
I^*	leakage current (A)
I_B	total current at the bipolar electrode (A)
L	electrode length (m)
N	number of experimental values in Equation 45
R	by-pass resistance (Ω)
U	applied voltage to the reactor (V)
U_0	reversible cell voltage (V)
W	electrode width (m)
x	axial coordinate (m)
y	axial coordinate (m)
z	normalized axial coordinate given by Equation 17

Greek characters

β	function given by Equation 18
γ	dimensionless number given by Equation 23
δ	normalized current density at the terminal electrodes given by Equation 16
δ_B	normalized current density at the bipolar electrode given by Equation 22
$\Delta\,\phi_{s,\,j}$	ohmic drop in the solution phase of the jth reactor (V)
$\eta_{i,\,j}$	overvoltage of the ith reaction (i = a or c) at the jth electrode (j = A, B or C) (V)
λ	dimensionless number given by Equation 24
ρ_s	electrolyte resistivity (Ωm)
φ	dimensionless number given by Equation 26
ω	dimensionless number given by Equation 25

Subscripts

A	terminal anode
B	bipolar electrode
C	terminal cathode
a	anodic reaction
c	cathodic reaction
s	solution phase

1. Introduction

Research in electrocatalysis has yielded activated electrodes which allow high current densities with very low overpotentials. As a consequence, feeding the current to achieve isopotentiality in the electrodes with the purpose of increasing their effectiveness has become more problematic. This effect can be minimized by the use of bipolar electrodes. Thus, there is a growing trend in industrial practice towards the use of bipolar arrangements. However, the use of electrochemical reactors with bipolar electrodes has drawbacks due to current leakage from cell to cell through the entry and exit ports. The leakage currents, also called parasitic or by-pass currents, cannot be avoided but they can be minimized by appropriate design.

Some researchers have analysed the design of bipolar electrolysers. Rousar and Cezner [1] considered a simplified model in which the individual cells and the inlet and outlet manifolds are replaced by a system of resistors in series and parallel. These authors worked with a non-divided reactor, which can be specifically applied to the production of sodium chlorate. The leakage currents were determined from the ohmic drop between platinum probes placed in the inlet and outlet channels of the electrolyte. Kuhn and Booth [2] carried out an early review. They emphasized the impact of the current losses in the design of industrial cells. In other works a pattern of resistors in series-parallel was considered and the influence of the number of cells, electrolyte resistivity and mathematical methods of solution on the leakage currents was discussed [3, 4]. Seiger [5] carried out experimental determinations of leakage currents in bipolar batteries formed by the silver oxide/zinc system. White et al. [6] predicted leakage currents in divided and non-divided bipolar reactors using circuit analog models. The potential distribution in the reactor, including the manifold region was presented [7]; here the Laplace equation for bipolar electrochemical reactors was solved by means of a numerical method assuming linear kinetics. Current distributions in chlor-alkali membrane cells were reported [8] taking into account the spatial dependence of the metal phase conductivities. Divisek et al. [9] computed the potential profile in electrolysers by numerical solution of the Laplace equation using the finite difference method. The potential profile was related to the potential-dependent thermodynamic stabilities of the respective metals in order to determine corrosion zones in the bipolar stack. Comninellis et al. [10] estimated leakage currents from polarization curves and compared these with experimental values obtained from measurement of the volume of gases evolved at the electrodes. At high current densities an acceptable agreement was found. Bonvin and Comninellis [11] reported that the by-pass current depends on two dimensionless numbers, one of them only depending on the electrochemical system and on the process parameters and the other only on the geometry of the reactor. This work is particularly useful for scale-up purposes. Bonvin et al. [12, 13] solved the Laplace equation using the finite element method for a bipolar electrochemical reactor and reported experimental results of current distributions. Rangarajan et al. [14] assumed Tafel kinetics and the complex system of equations was solved by means of different methods.

The influence of leakage currents on the current distribution at each electrode has been scarcely analysed in the literature. Non-uniform current distribution may affect membranes and catalyst coating life.

The present work develops a model for the prediction of current density distribution and determines the main dimensionless groups which define the distribution. In order to determine the predictive capability of the mathematical treatment, comparisons between calculated and experimental primary current distributions are performed.

2. Mathematical model

2.1. *General treatment*

The electrochemical reactor is the simple case of one bipolar element between two feeder electrodes and the configuration is sketched in Figure 1. Considering the symmetry of the arrangement, only one half of the reactor is shown. The overall voltage balance at the axial position y may be written as

$$U = 2\,U_0 + \eta_{a,A}\left[j_{a,A}(y)\right] + \Delta\phi_{s,1}(y) + \eta_{c,B}\left[j_{c,B}(y)\right] + \eta_{a,B}\left[j_{a,B}(y)\right] + \Delta\phi_{s,2}(y) + \eta_{c,C}\left[j_{c,C}(y)\right] \quad (1)$$

assuming

$$j_{a,A}(y) = j_{c,C}(y) = j(y) \quad (2)$$

and

$$j_{a,B}(y) = j_{c,B}(y) = j_B(y) \quad (3)$$

Tafelian kinetics are assumed

$$\eta = b[\ln(j) - \ln(j_0)] \quad (4)$$

Considering that the supply and discharge nozzles for the electrolyte are in the middle of the interelectrode gap the ohmic drop in the solution phase is given by

$$\Delta\phi_{s,1}(y) = \Delta\phi_{s,2}(y) = \rho_s e/2 j(y) + \rho_s e/2 j_B(y) \quad (5)$$

Introducing Equations 2–5 into Equation 1 and rearranging yields

$$(b_a + b_c)\ln[j(y)] + (b_a + b_c)\ln[j_B(y)] + \rho_s e[j(y) + j_B(y)] = C_1 \quad (6)$$

where

$$C_1 = U - 2\,U_0 + 2\,b_a \ln\left(j_{0,a}\right) + 2\,b_c \ln\left(j_{0,c}\right) \quad (7)$$

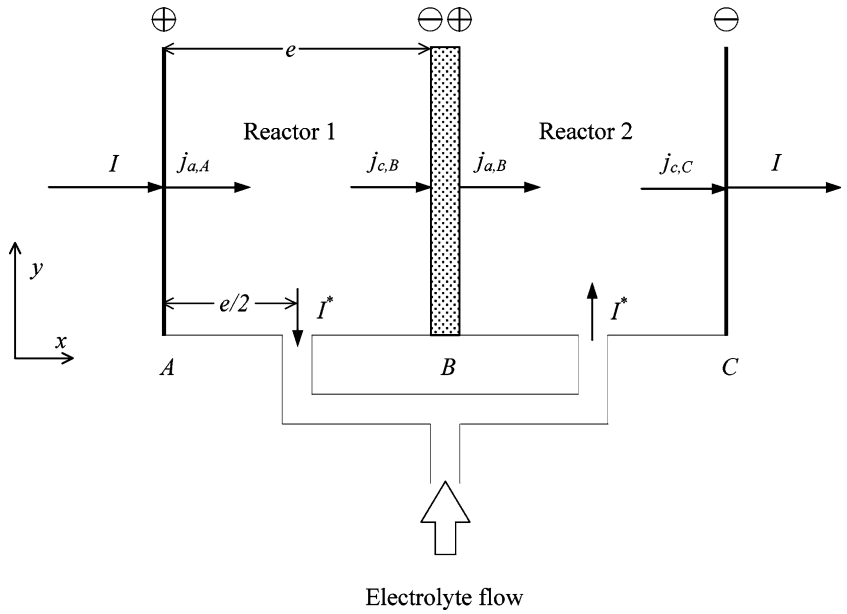

Fig. 1. Geometry of the model.

The voltage balance at the axial position y including the inlet manifold of the electrolyte is

$$U = U_0 + \eta_{a,A}\left[j_{a,A}(y)\right] + \Delta\phi_{s,1}(y)\big|_0^{e/2} + \Delta\phi_{s,1}(y)\big|_y^0 + \frac{\rho_s G}{A} I^* + \Delta\phi_{s,2}(y)\big|_0^y + \Delta\phi_{s,2}(y)\big|_{e/2}^e + \eta_{c,C}\left[j_{c,C}(y)\right] \tag{8}$$

where

$$\Delta\phi_{s,1}\big|_0^{e/2} = \Delta\phi_{s,2}\big|_{e/2}^e = \rho_s \frac{e}{2} j(y) \tag{9}$$

According to the schematic representation of Figure 2 the differential current balance in the solution phase is

$$\frac{dj_s(y)}{dy} = -\frac{1}{e}[j(y) - j_B(y)] \tag{10}$$

Combining Equation 10 with the Ohm's law for the solution phase and integrating yields

$$\Delta\phi_{s,1}\big|_y^0 = \Delta\phi_{s,2}\big|_0^y = \frac{\rho_s I^*}{We} y - \frac{\rho_s}{e} \int_0^y \int_0^y [j(y) - j_B(y)]dydy \tag{11}$$

Introducing Equations 4, 9 and 11 into Equation 8 and rearranging gives

$$(b_a + b_c)\ln[j(y)] + \rho_s e j(y) + \frac{\rho_s G}{A} I^* + \frac{2\rho_s I^*}{We} y - \frac{2\rho_s}{e} \int_0^y \int_0^y [j(y) - j_B(y)]dydy = C_2 \tag{12}$$

where

$$C_2 = U - U_0 + b_a \ln\left(j_{0,a}\right) + b_c \ln\left(j_{0,c}\right) \tag{13}$$

Evaluating Equation 12 at $y = 0$ gives

$$(b_a + b_c)\ln[j(0)] + \rho_s e j(0) + \frac{\rho_s G}{A} I^* = C_2 \tag{14}$$

Combining Equations 12 and 14 and rearranging yields

$$[\delta(z) - 1] + \gamma \ln[\delta(z)] = -\beta(z) \tag{15}$$

where the following dimensionless variables were introduced

$$\delta(z) = \frac{j(z)}{j(0)} \tag{16}$$

$$z = \frac{y}{L} \tag{17}$$

and

$$\beta(z) = \lambda\left(\omega z - \int_0^z \int_0^z \delta dz\, dz + \varphi \int_0^z \int_0^z \delta_B dz\, dz\right) \tag{18}$$

Combining Equations 12 and 6 gives

$$(b_a + b_c)\ln[j_B(y)] + \rho_s e j_B(y) = = C_1 - C_2 + \frac{\rho_s G}{A} I^* + \frac{2\rho_s I^*}{We} y - \frac{2\rho_s}{e} \int_0^y \int_0^y [j(y) - j_B(y)]dy\, dy \tag{19}$$

Evaluating Equation 19 at $y = 0$ gives

$$(b_a + b_c)\ln[j_B(0)] + \rho_s e j_B(0) = C_1 - C_2 + \frac{\rho_s G}{A} I^* \tag{20}$$

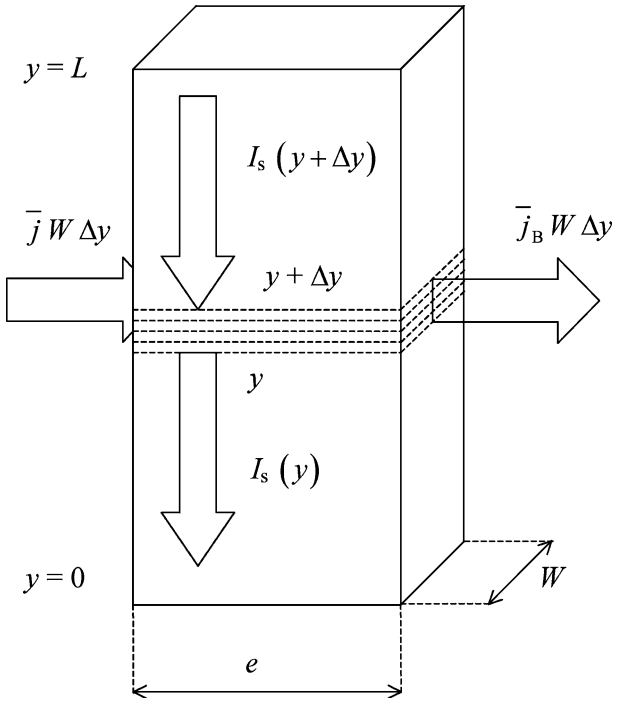

Fig. 2. Schematic representation of the current flows in the electrolyte.

Combining Equations 19 and 20 and rearranging, in terms of z, yields

$$[\delta_B(z) - 1] + \frac{\gamma}{\varphi}\ln[\delta_B(z)] = \frac{\beta(z)}{\varphi} \tag{21}$$

where

$$\delta_B(z) = \frac{j_B(z)}{j_B(0)} \tag{22}$$

The current distributions in the terminal and bipolar electrodes are given by Equations 15 and 21, respectively. The parameters introduced in the above equations are defined as

$$\gamma = \frac{(b_a + b_c)}{\rho_s\, e\, j(0)} \tag{23}$$

γ represents a Wagner number [15], where the polarization resistance takes into account the Tafel slopes of both electrochemical reactions and is evaluated for the total current at $z = 0$.

$$\lambda = \frac{2L^2}{e^2} \tag{24}$$

$$\omega = \frac{I^*}{L\,W j(0)} \tag{25}$$

and

$$\varphi = \frac{j_B(0)}{j(0)} \tag{26}$$

Combining Equations 15 and 21 yields

$$(\delta - 1) + \varphi\,(\delta_B - 1) + \gamma \ln(\delta\,\delta_B) = 0 \tag{27}$$

The product $\delta\delta_B$ approaches unity. Thus, Equation 27 is simplified to

$$[\delta(z) - 1] \cong -\varphi\,[\delta_B(z) - 1] \tag{28}$$

Therefore, a linear relationship may be expected when $(\delta - 1)$ is plotted as a function of $(\delta_B - 1)$.

For a given value of reactor applied voltage the leakage current can be obtained by combining Equations 14 and 23

$$I^* = \frac{A\,e\,j(0)}{G}\left\{\frac{C_2}{\rho_s e j(0)} - 1 - \gamma \ln[j(0)]\right\} \tag{29}$$

The total currents at the terminal and bipolar electrodes are respectively given by

$$I = j(0)\,W L \int_0^1 \delta(z)\mathrm{d}z \tag{30}$$

and

$$I_B = j_B(0)\,W L \int_0^1 \delta_B(z)\mathrm{d}z \tag{31}$$

2.2. *Simplified treatment*

Assuming that

$$\int_0^z \int_0^z \delta\,\mathrm{d}z\,\mathrm{d}z \cong \int_0^z \int_0^z \delta_B\,\mathrm{d}z\,\mathrm{d}z \tag{32}$$

Equation 18 yields

$$\beta(z) = \lambda\left[w\,z - (1 - \varphi)\int_0^z \int_0^z \delta\,\mathrm{d}z\,\mathrm{d}z\right] \tag{33}$$

For values of δ near to one for all z, Equation 33 simplifies to

$$\beta(z) = \lambda\left[\omega\,z - (1 - \varphi)\frac{z^2}{2}\right] \tag{34}$$

Likewise, from Equations 30 and 31 and taking into account Equation 32 gives

$$[j(0) - j_B(0)]\,W L \cong 2\,I^* \tag{35}$$

Combining Equations 25, 26, 34 and 35 gives

$$\beta(z) = \lambda\,\omega\left(z - z^2\right) \tag{36}$$

Introducing Equation 36 into Equations 15 and 21 yields

$$[\delta(z) - 1] + \gamma\,\ln[\delta(z)] = -\lambda\,\omega\left(z - z^2\right) \tag{37}$$

and

$$[\delta_B(z) - 1] + \frac{\gamma}{\varphi}\ln[\delta_B(z)] = \frac{\lambda\,\omega}{\varphi}\left(z - z^2\right) \tag{38}$$

2.3. *Primary current distributions*

The primary current distributions can be obtained as a limiting case of the above mathematical treatment when $\gamma \to 0$. Therefore, the main equations are

$$[\delta(z) - 1] = -\beta(z) \tag{39}$$

and

$$[\delta_B(z) - 1] = \frac{\beta(z)}{\varphi} \tag{40}$$

According to Equation 27 the relationship between the two distributions is given by

$$[\delta(z) - 1] = -\varphi\,[\delta_B(z) - 1] \tag{41}$$

For the simplified model case, taking into account Equations 37 and 38, the primary current distributions show a parabolic function with position according to

$$\delta(z) = 1 - \lambda\,\omega\left(z - z^2\right) \tag{42}$$

and

$$\delta_B(z) = 1 + \frac{\lambda\,\omega}{\varphi}\left(z - z^2\right) \tag{43}$$

According to Equation 29 and taking into account that for primary distribution $C_2 = U$, the leakage current is

$$I^* = \frac{1}{R}[U - \rho_s\, e\, j(0)] \tag{44}$$

3. Theoretical predictions according to the simplified model

The following results correspond to the iterative solution of Equations 37 and 38. Figures 3 and 4 show the effect of the transverse section and length of the electrolyte manifold on the current distributions. As A increases and G decreases the current distributions are more non-uniform because of the increase in leakage current. It must be emphasized that A and G have an indirect effect on the current distributions by means of their influence on the leakage current.

Figure 5 shows the effect of the dimensionless parameter λ on the current distributions for a given value of γ. The decrease in interelectrode gap gives an increase in λ and the current distribution becomes more uneven. This behaviour can be understood taking into account that the increase in e increases the flow area for I^* inside the reactor. Then the regions of electrode far from the inlet have a smaller resistance to contribute to the leakage current. Thus, the current distribution is more uniform. In contrast, when e is very small only the electrode areas near to the inlet region can contribute to I^* causing uneven current distributions. Figure 5 also shows that the current distribution is more uniform when the electrode length decreases, because for longer electrodes the regions far from the electrolyte inlet do not contribute to the leakage current.

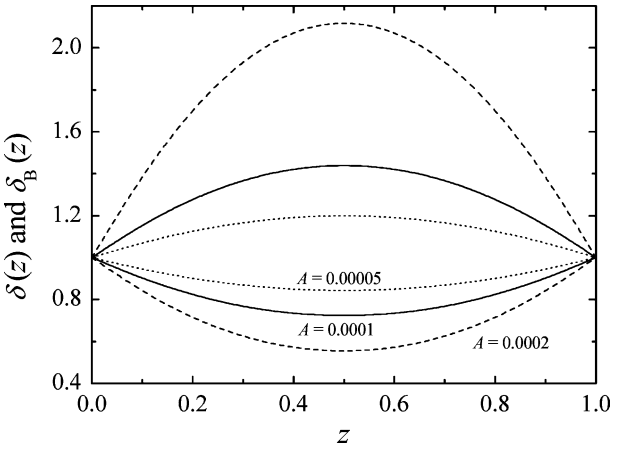

Fig. 3. Current distributions for different values of the transverse section of the electrolyte manifold. Upper curves: bipolar electrode. Lower curves: terminal electrodes.

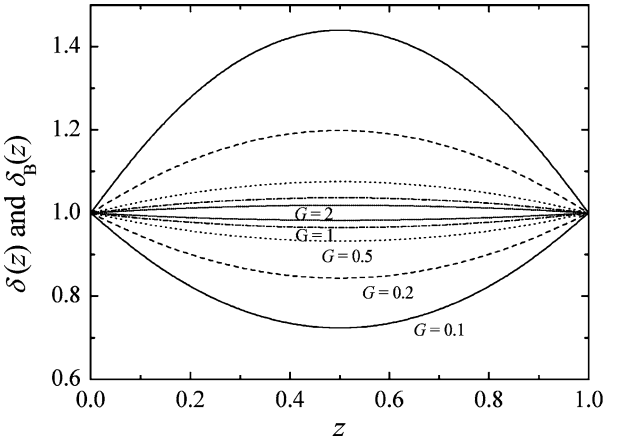

Fig. 4. Current distributions for different values of electrolyte manifold length. Upper curves: bipolar electrode. Lower curves: terminal electrodes.

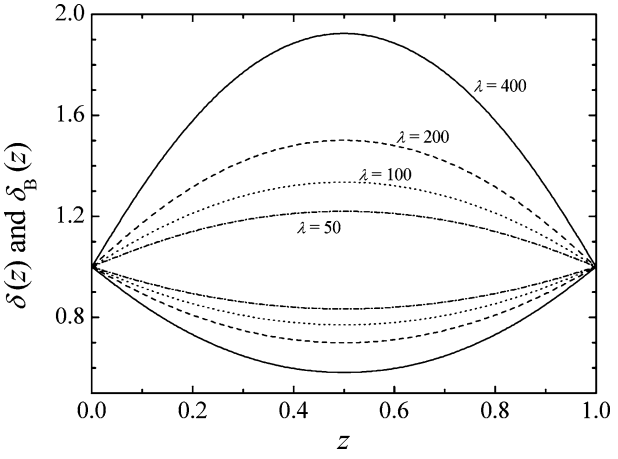

Fig. 5. Current distributions as a function of the dimensionless parameter λ. Upper curves: bipolar electrode. Lower curves: terminal electrodes. $\gamma = 0.1$.

Figure 6 shows the effect of the dimensionless parameter γ on the current distributions for a given value of λ. The current distributions become more uniform for lower values of γ which can be explained taking into account that for low values of γ the polarization resistance at the bipolar electrode are smaller than the electrolyte resistance in the solution manifolds. Thus, the leakage current is small and the current distributions more uniform.

Figure 7 shows the combined effects of γ and λ on the dimensionless current φ, which represents a measurement of the current distribution in the reactor. Clearly, Figure 7 confirms that a decrease in both γ and λ makes the current distribution more uniform due to the fact that φ approaches unity.

Figure 8 shows the combined effect of γ and λ on the leakage current related to the total current. As expected, the ratio between the currents decreases when λ increases and γ decreases.

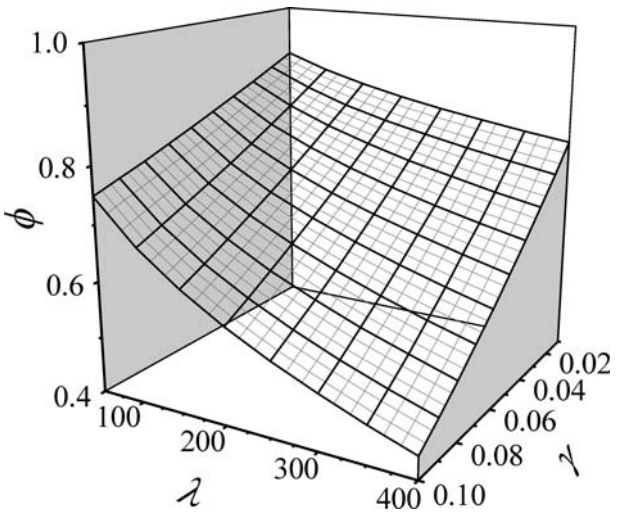

Fig. 7. Current density at $y = 0$ for the bipolar electrode related to the current density at $y = 0$ for the terminal electrodes as a function of the dimensionless parameters γ and λ.

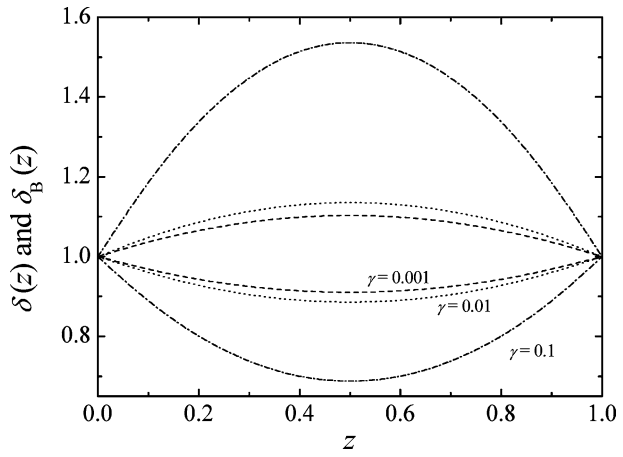

Fig. 6. Current distributions as a function of the dimensionless parameter γ. Upper curves: bipolar electrode. Lower curves: terminal electrodes. $\lambda = 200$.

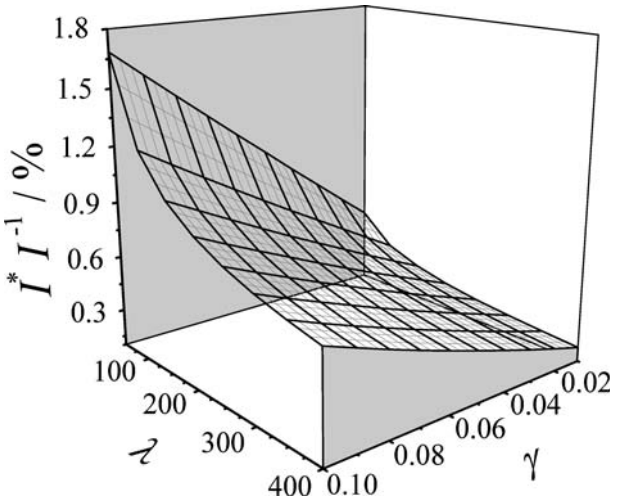

Fig. 8. Leakage current related to the total current as a function of the dimensionless parameters γ and λ.

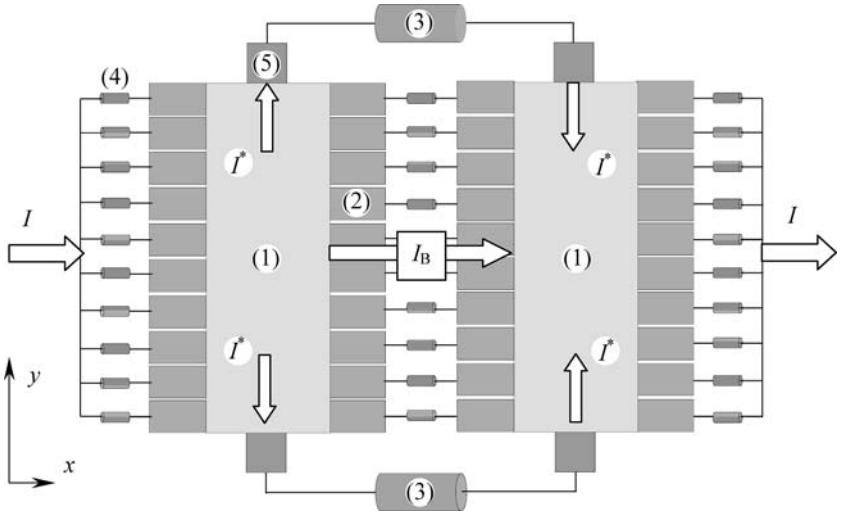

Fig. 9. Schematic view of the experimental arrangement. (1) conductive paper, (2) segmented electrodes, (3) by-pass resistors, (4) resistors, (5) electric contact.

4. Comparison with experimental results of primary current distribution

4.1. *Experimental*

In order to measure the primary current distributions, each module of the bipolar electrochemical reactor was simulated by a sheet of conductive paper (Pasco Scientific, PK 9025) mounted on a non-conducting board and the electrodes were formed by ten copper segments, 9.5×10^{-3} m wide, at opposite sides of the conductive paper. The segments were insulated from one another by an approximately 5×10^{-4} m thickness Teflon slide. A calibrated resistor, approximately 1 Ω resistance, was intercalated between each segment and the current feeder of the electrodes. The current distribution was determined by measuring the ohmic drop in the corresponding resistor. The interelectrode gap was 0.02 m and the conductive paper and segments were trimmed to give a reactor length of 0.1 m. The thickness of the conductive paper was 1.3×10^{-4} m and the resistivity was 5.02 Ωm. The inlet and outlet manifolds were also simulated by by-pass resistors. Figure 9 depicts the arrangement. A dc power supply was used to apply a constant current to the feeders.

4.2. *Results and discussion*

Figure 10 shows the current at each segment as a function of position when the system is operated without by-pass resistors. As expected the current oscillates around the mean value. This behaviour can be understood taking into account that the system is very sensitive to the contact resistance between the conductive paper and the segments.

Figure 11 shows typical curves of current distribution at the terminal and bipolar electrodes for different resistance values of the by-pass resistor. The theoretical predictions according to Equations 42 and 43, in terms of current density, are also given. It can be observed that, at the terminal electrodes, for the highest resistance values in the by-pass resistor, there is a close agreement between the experimental and theoretical data. However, for the bipolar electrode the theoretical primary current distribution is more pronounced than the experimental one. Figure 11 shows that for a given current the current distributions become more uneven when the by-pass resistance decreases, due to the increase in leakage current.

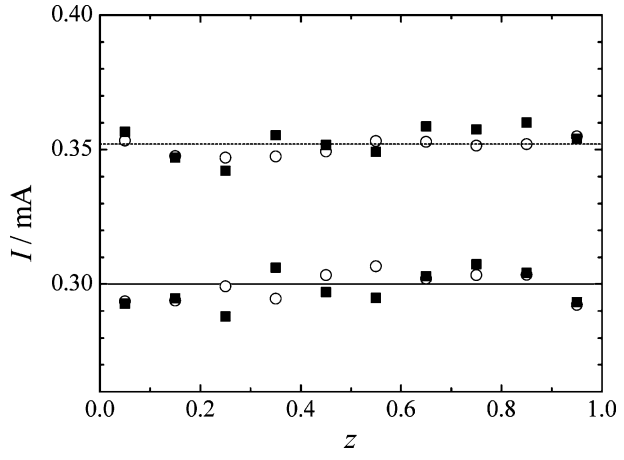

Fig. 10. Current as a function of position for the system without by-pass. Full line: I = 3 mA. Dotted line: I = 3.52 mA. (○) Terminal electrodes. (■) Bipolar electrode.

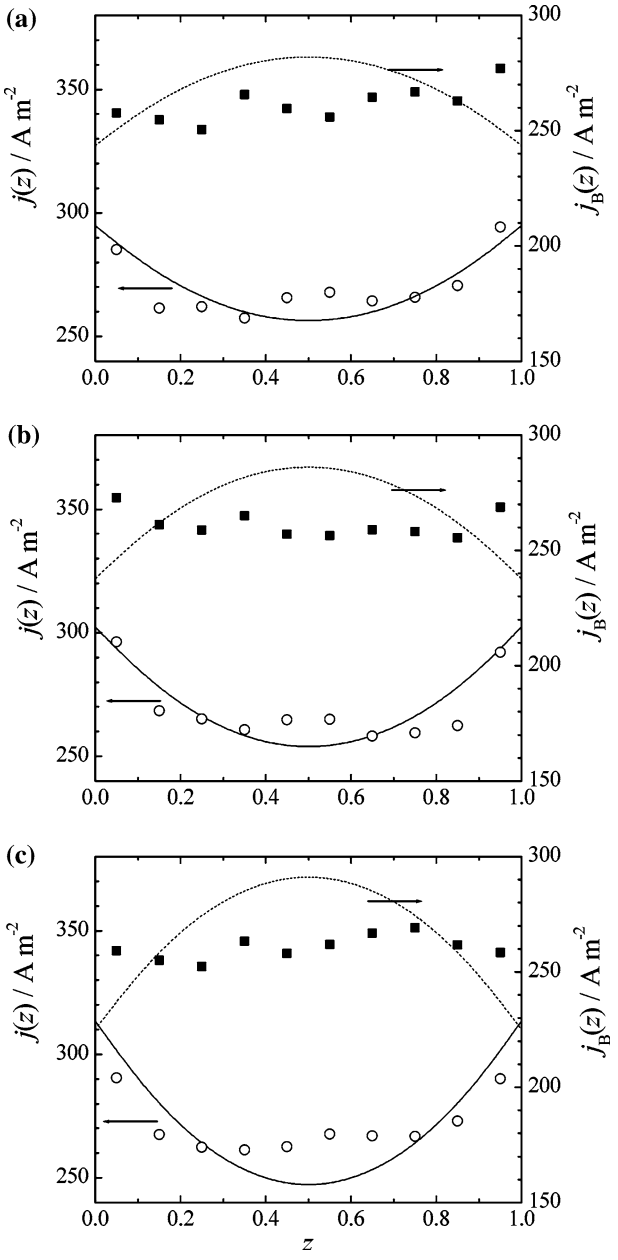

Fig. 11. Primary current density distributions. I = 3.5 mA. (a) R = 605658 Ω, (b) R = 468380 Ω and (c) R = 324254 Ω. (○) experimental data for the terminal electrodes. Full line: theoretical prediction for the terminal electrodes, Equation 42 in terms of current density. (■) experimental data for the bipolar electrode. Dotted line: theoretical prediction for the bipolar electrode, Equation 43 in terms of current density.

Table 1. Summary of typical experimental results

R/Ω	I/mA	$\overline{d}_r$/%			Theoretical values	Experimental values	Error/%
		Terminal	Bipolar				
63228	2.00	11.46	17.52	U/V	30.90	28.01	9.35
				I^*/mA	0.1212	0.1161	4.21
	3.00	11.44	17.78	U/V	46.35	41.86	9.69
				I^*/mA	0.1818	0.1861	2.37
	3.51	11.49	17.85	U/V	54.23	49.13	9.40
				I^*/mA	0.2127	0.2203	3.57
324254	2.00	3.67	7.03	U/V	30.90	29.96	3.04
				I^*/mA	0.0398	0.0356	10.55
	3.00	3.62	7.08	U/V	46.35	45.07	2.76
				I^*/mA	0.0597	0.0563	5.70
	3.50	3.90	6.70	U/V	54.08	51.13	5.45
				I^*/mA	0.0697	0.0671	3.73
605658	2.00	2.43	5.15	U/V	30.90	33.58	8.67
				I^*/mA	0.0231	0.0283	22.51
	3.00	2.29	5.44	U/V	46.35	50.06	8.00
				I^*/mA	0.0346	0.0475	37.28
	3.50	2.18	5.40	U/V	54.08	58.11	7.45
				I^*/mA	0.0404	0.0520	28.71

Table 1 summarizes the results. In columns 3 and 4, the mean relative deviation $\overline{d}_r$, defined as:

$$\overline{d}_r = \frac{1}{N}\sum_{i=1}^{N}\frac{\left|j_{exp}(z_i) - j_{th}(z_i)\right|}{j_{th}(z_i)}100 \qquad (45)$$

is given. For the terminal electrodes, $\overline{d}_r$ is low showing that the mathematical treatment is reliable for the calculations of primary current distribution. However, when the by-pass resistance decreases a greater discrepancy, higher $\overline{d}_r$, between the theoretical and experimental distributions is observed. Columns 6 and 7 also compare the experimental values of the cell voltages and leakage currents with the theoretical predictions and an acceptable predictive capability of the model is evident.

5. Conclusions

(i) The simplified theoretical model shows that leakage currents produce uneven current distributions in the reactor. Thus, for the bipolar electrode a maximum in the current density at the central part is predicted and for the terminal electrodes at the inlet and outlet regions. The current distributions depend on two dimensionless numbers. One corresponds to a Wagner number, γ, and the other, λ, characterizes the geometry of the system. The effect of leakage current on current distribution is more pronounced when both γ and λ increase.

(ii) The mathematical model satisfactorily predicts the primary current distributions at the terminal electrodes for the highest resistance values. For a given current the model is also appropriate for the calculation of leakage current and cell voltage. Thus, the reported theoretical treatment is a helpful tool to perform a simplified first analysis of the performance of bipolar electrochemical reactors.

Acknowledgements

This work was supported by the Agencia Nacional de Promoción Científica y Tecnológica (ANPCyT), Consejo Nacional de Investigaciones Científicas y Técnicas (CONICET) and Universidad Nacional del Litoral (UNL) of Argentina.

References

1. I. Rousar and V. Cezner, *J. Electrochem. Soc.* **121** (1974) 648.
2. A.T. Kuhn and J.S. Booth, *J. Appl. Electrochem.* **10** (1980) 233.
3. W. Thiele, M. Schleiff and H. Matschiner, *Electrochim. Acta* **26** (1981) 1005.
4. E.A. Kaminski and R.F. Savinell, *J. Electrochem. Soc.* **130** (1983) 1103.
5. H.N. Seiger, *J. Electrochem. Soc.* **133** (1986) 2002.
6. R.E. White, C.W. Walton, H.S. Burney and R.N. Beaver, *J. Electrochem. Soc.* **133** (1986) 485.
7. E.C. Dimpault-Darcy and R.E. White, *J. Electrochem. Soc.* **135** (1988) 656.
8. R.E. White, F. Jagush and H.S. Burney, *J. Electrochem. Soc.* **137** (1990) 1846.
9. J. Divisek, R. Jung and D. Britz, *J. Appl. Electrochem.* **20** (1990) 186.
10. Ch. Comninellis, E. Plattner and P. Bolomey, *J. Appl. Electrochem.* **21** (1991) 415.
11. G. Bonvin and Ch. Comninellis, *J. Appl. Electrochem.* **24** (1994) 469.
12. G. Bonvin, Ch. Comninellis and E. Plattner, 43rd ISE Meeting Abstract Book, 3–21, (1992).
13. G. Bonvin, Swiss Federal Institute of Technology, Lausanne, thesis 1029 (1992).
14. S.K. Rangarajan and V. Yegnanarayanan, *Electrochim. Acta* **42** (1997) 153.
15. C. Wagner, *J. Electrochem. Soc.* **98** (1951) 116.